Pseudomonas aeruginosa expresses a functional human natriuretic peptide receptor ortholog: involvement in biofilm formation

Thibaut Rosay[1], Alexis Bazire[2], Suraya Diaz[3], Thomas Clamens[1], Anne-Sophie Blier[1], Lily Mijouin[1], Brice Hoffmann[4], Jacques-Aurélien Sergent[5], Emeline Bouffartigues[1], Wilfrid Boireau[6], Julien Vieillard[7], Christian Hulen[1], Alain Dufour[2], Nicholas J. Harmer[3], Marc G.J. Feuilloley[1] and Olivier Lesouhaitier[1]*

[1]*Laboratory of Microbiology Signals and Microenvironment LMSM EA 4312, University of Rouen, 27000 Evreux, France*

[2]*Univ. Bretagne-Sud, EA 3884, LBCM, IUEM, F-56100 Lorient, France*

[3]*School of Biosciences, University of Exeter, Exeter, EX4 4QD, UK*

[4]*IMPMC, UMR7590, CNRS, Université Pierre et Marie Curie - Paris 6, 4 place Jussieu, F75252, Paris Cedex 05, France*

[5]*Department of Biology, University of Cergy-Pontoise, Cergy-Pontoise, France*

[6]*Institut FEMTO-ST, Université de Franche Comté, CLIPP, Besançon, France*

[7]*UMR CNRS 6014 COBRA, University of Rouen, 27000 Evreux, France*

* Corresponding author: Olivier Lesouhaitier, olivier.lesouhait@univ-rouen.fr

Running title: AmiC sensor acts as a bacterial hormone receptor

Key words: Cystic fibrosis; Lung; Natriuretic peptides; NPR-C; AmiC; Biofilm; Bacterial adaptation; Microscale thermophoresis

Abstract

Considerable evidence exists that bacteria detect eukaryotic communication molecules and modify their virulence accordingly. In previous studies, it has been demonstrated that the increasingly antibiotic resistant pathogen *Pseudomonas aeruginosa* can detect the human hormones Brain Natriuretic peptide (BNP) and C-type Natriuretic Peptide (CNP) at micromolar concentrations. In response, the bacterium modifies its behavior to adapt to the host physiology, increasing its overall virulence. Identifying the bacterial sensor for these hormones and interfering with this sensing mechanism offers an exciting opportunity to directly affect the infection process.

Here, we show that BNP and CNP strongly decrease *P. aeruginosa* biofilm formation. Isatin, an antagonist of human natriuretic peptide receptors (NPR), prevents this effect. Furthermore, the human NPR-C receptor agonist $cANF^{4-23}$ mimics the effects of natriuretic peptides on *P. aeruginosa* while sANP, the NPR-A receptor agonist, appears weakly active. We show *in silico* that NPR-C, a preferential CNP receptor, and the *P. aeruginosa* protein AmiC have similar 3D structures, and that both CNP and isatin bind to AmiC. We demonstrate that CNP acts as an AmiC agonist, enhancing the expression of the *ami* operon in *P. aeruginosa*. Binding of CNP and NPR-C agonists to AmiC was confirmed by microscale thermophoresis. Finally, using an *amiC* mutant strain, we demonstrate that AmiC is essential for CNP effects on biofilm formation.

In conclusion, the AmiC bacterial sensor possesses similar structural and pharmacological profiles to the human NPR-C receptor and appears to be a bacterial receptor for human hormones that enables *P. aeruginosa* to modulate biofilm expression.

Importance

Pseudomonas aeruginosa is a bacterium that is a highly dangerous opportunist pathogen for immunocompromised hosts, especially cystic fibrosis patients. The sites of *P. aeruginosa* infection are varied, with predominance in the human lung, in which bacteria are in contact with host molecular messengers such as hormones. The C-type natriuretic peptide (CNP), a hormone produced by lung cells, has been described as a bacterial virulence enhancer. In this report, we showed that the CNP hormone counteracts *P. aeruginosa* biofilm formation and we identified the bacterial protein AmiC as the sensor involved in the CNP effects. We showed that AmiC could bind specifically CNP. These results show for the first time that a human hormone could be sensed by bacteria through a specific protein which is an ortholog of the human hNPR-C. The bacterium would be able to modify its lifestyle by favoring virulence factors production whilst reducing biofilm formation.

INTRODUCTION

Pseudomonas aeruginosa is a well known opportunistic pathogen and a major cause of mortality among cystic fibrosis patients (1). The morbidity of this bacterium and its resistance to antibiotherapy are largely attributed to its transition in host tissues (particularly in lung, soft tissues, skin and urinary bladder) from a planktonic to a biofilm lifestyle (2, 3). The present emergence of multi-resistant strains is now critical and is prompting the need to find new therapeutic approaches (4).

The high adaptability of *P. aeruginosa* and its rapid response to the host environment implies that it can detect a large range of eukaryotic chemical signals (5). However, few bacterial sensors for eukaryotic molecules have been characterized to date (6). Studies on the *E. coli* quorum-sensing regulator A (QseA) led to the identification of QseC/QseB, a two-component regulatory system (7, 8). This system is not only activated by the bacterial quorum sensing signal autoinducer AI3, but also by eukaryotic neurohormones (epinephrine/norepinephrine) (9). It was suggested that QseC could be a bacterial ortholog of eukaryotic adrenergic receptors (10). Bioinformatic screening of *E. coli* QseC analogs has demonstrated the presence of proteins related to this sensor in a large number of bacterial pathogens, including *P. aeruginosa* (11), in which norepinephrine acts as a virulence inducer (12). It appears that *P. aeruginosa* is able to sense different eukaryotic communication molecules, including interferon-γ (13), dynorphin (14), gamma aminobutyric acid (GABA) (15) and natriuretic peptides (16, 17).

Natriuretic peptides are a family of eukaryotic hormones and neurohormones composed of three members, atrial natriuretic peptide (ANP), brain natriuretic peptide (BNP) and C-type natriuretic peptide (CNP). These peptides are mainly expressed in cardiomyocytes and endothelial cells (18) explaining their major role in cardiovascular homeostasis. However,

ANP and CNP are also produced in significant amounts by the lung bronchial and alveolar epithelia and particularly by Clara (Club) cells (19). The circulating blood levels of natriuretic peptides are increased during community-acquired pneumonia (20), and the lipopolysaccharides (LPS) of Gram-negative bacteria induce the plasmatic release of both BNP (21) and CNP (22). In previous studies, we demonstrated that *P. aeruginosa* can detect BNP and CNP at micromolar concentrations and reacts by an overall increase of virulence (16, 17). In *P. aeruginosa*, the effect of CNP appears to be mediated by cAMP synthesis, which subsequently activates the regulatory proteins Vfr (17) and PtxR (16), leading to a rise of HCN and exotoxin A production and a reorganization of LPS structure. For these reasons, it was suggested that CNP promotes the acute infection phenotype of *P. aeruginosa* (23), favoring the switch of *P. aeruginosa* towards a planktonic lifestyle, and a decrease in biofilm formation. The effects of BNP and CNP on *P. aeruginosa* appear to be mediated by distinct mechanisms since BNP, unlike CNP, did not modify intra-bacterial cAMP levels (17) and was without effect on *P. aeruginosa* virulence towards *C. elegans* (16). In humans, each type of natriuretic peptide acts through a particular receptor subtype, suggesting the expression of specific bacterial orthologs of the human natriuretic peptide receptors in *P. aeruginosa*.

In the present study, we extended our knowledge of the effect of natriuretic peptides on *P. aeruginosa* by investigating for the first time the effect of these peptides on the biofilm formation activity of the bacterium. Using *in silico* approaches, we identified the *P. aeruginosa* protein AmiC as a potential CNP binding sensor site and investigated *in vitro* the binding of natriuretic peptide receptor agonists to AmiC. The pharmacological profile of AmiC as a bacterial CNP receptor was completed by studying the effect of isatin, an antagonist of human CNP receptors that is also a known bacterial metabolite and signaling compound. We further determined the affinity of AmiC for several natriuretic peptide receptor agonists. Using an *amiC* deficient mutant and its complemented derivative, we

validated the crucial role of *P. aeruginosa* AmiC in the effect of CNP, but not BNP, on biofilm formation. This study provides an integrated explanation of the CNP sensing system in *P. aeruginosa* and opens up the way to a new strategy to control *P. aeruginosa* biofilm formation.

RESULTS

Effects of CNP and BNP on *P. aeruginosa* biofilm formation.

The influence of CNP and BNP on the biofilm formation activity of *P. aeruginosa* was investigated in dynamic and static conditions. Unless otherwise stated, peptides were used at a micromolar concentration since *i)* this corresponds to that usually used for studying the effects of peptides on eukaryotic models (24), *ii)* they were previously shown to be active at this concentration on quorum sensing molecules and toxin productions in *P. aeruginosa* (16), and *iii)* the duration of the biofilm experiment, which required a high amount of medium (continuous flow) containing the peptides, was not compatible with the realization of a whole dose response study. When *P. aeruginosa* PA14 was exposed to CNP or BNP in dynamic conditions, we observed a highly significant decrease of the biofilm volume (-81.0 ± 6.6% and -80.3 ± 4.4%, $p < 0.001$, respectively) and of the biofilm average thickness (-72.3 ± 9.7% and -76.0 ± 4.8%, $p < 0.001$, respectively) (Fig. 1A). These effects were associated with a reduction of the number and mean size of mushroom-like structures in the biofilm (Fig. 1B). Exposure of *P. aeruginosa* MPAO1 to CNP for 24 h in static conditions led to similar results with a marked decrease of biofilm formation (Fig. 2A) associated to a reduction of volume and thickness (-83.3 ± 1.9% and -91.7 ± 2.2% , $p < 0.001$, respectively) (Fig. 2B).

Effect of specific antagonist and agonists of natriuretic peptide receptors on *P. aeruginosa* biofilm formation and virulence activity.

The biofilm formation activity of *P. aeruginosa* MPAO1 was also studied in the presence of isatin, an antagonist of both A and C subtypes natriuretic peptide receptors (NPR-A and NPR-C). Administered alone for 24 h, isatin affected the organization of the biofilm which appeared more irregular with the presence of large water channels (Fig. 2A). We also noted a limited and non-significant increase of the biomass and thickness of the biofilm (Fig. 2B).

However, when *P. aeruginosa* MPAO1 was exposed to isatin (10^{-5} M) for 20 min prior to the administration of CNP, the inhibitory effect of CNP on the biofilm formation activity of the bacterium was abolished (Fig. 2A and 2B).

As we have previously shown that natriuretic peptides enhance *P. aeruginosa* cytotoxicity activity and global virulence (16), we tested the effect of sANP, a specific NPR-A agonist, and the artificial peptide $cANF^{4-23}$, a specific NPR-C agonist, on bacterial cytotoxicity towards lung cells. The peptide $cANF^{4-23}$ (NPR-C agonist) caused a strong increase of *P. aeruginosa* cytotoxicity activity against A549 human lung epithelial cells (+ 98.3 ± 16.9%; $p < 0.001$) (Fig. 2C). In parallel, we observed that the sANP peptide (NPR-A agonist), also enhanced the *P. aeruginosa* cytotoxicity in the same cell model, but to a lower extent (+ 25.9 ± 12.1%; $p < 0.05$) (Fig. 2C).

In silico study of a functional C-type natriuretic peptide receptor ortholog in _P. aeruginosa_.

In mammalian cells, CNP preferentially binds the NPR-C receptor and has a weak affinity for the NPR-A receptor (25), whereas BNP strongly binds NPR-A and has a weak affinity for NPR-C. The observations that the effects of CNP were blocked by the NPR-C antagonist isatin, and mimicked by the NPR-C agonist $cANF^{4-23}$, suggested the presence of a bacterial ortholog of NPR-C in *P. aeruginosa*. This hypothesis was investigated using *in silico* approaches. Searching in bibliographic data, we noted a DALI structure similarity search (26) that identified a *P. aeruginosa* protein, AmiC, which shows structural homologies with the binding domain of natriuretic peptides receptors (27, 28). Using tools from the Protein Data Bank in Europe [http://www.ebi.ac.uk/pdbe/], we investigated in detail the structure of *P. aeruginosa* AmiC bound to its known ligand acetamide. We observed that it shares high structural similarity with the natriuretic peptide receptor subtype NPR-C bound to one of its

agonists, the atrial natriuretic peptide (ANP; *data not shown*). This supports the hypothesis that AmiC could act as a bacterial natriuretic peptide sensor.

The 3D structure of *P. aeruginosa* AmiC (PDB ID: 1PEA) (29) was compared to that of the human NPR-C receptor (hNPR-C) (PDB ID: 1JDP) (30). Using the STAMP software (31), we superimposed an AmiC monomer onto each protomer of the structure of an hNPR-C dimer in complex with CNP. Although the sequences of these proteins share only 19% identity and 26% similarity, these two proteins present an overall similar 3D structure in the homodimeric form (Fig. 3A), particularly at the interface between each monomer which is considered to be the binding cleft of hNPR-C. The highest similarity was found in the helix of AmiC corresponding to the region involved in the binding of CNP to hNPR-C. Next, we split the AmiC monomer into two parts, corresponding to the two lobes of the protein. The first lobe consists of amino acids 8 to 123 and 261 to 338, and the second lobe of amino acids 124 to 260 and 339 to 375 of AmiC. Then, we superimposed each lobe on the 3D structure of hNPR-C (Fig. 3B). Each lobe of hNPR-C and AmiC showed a high level of secondary structure conservation with similar 3D positions, reinforcing the concept of structural homology between these two proteins. Using GASH Structural Superposition software (32) on each lobe of hNPR-C and AmiC, we observed that each of these two proteins has 254 residues estimated to be involved in equivalent secondary structures, covering 61.7% of the AmiC sequence. The hinge between the two lobes was essentially formed with flexible loops. Once superimposed, we looked at the amino acids involved in the binding of CNP, supporting the hypothesis that AmiC and hNPR-C bind the peptide in a similar fashion. Supplemental material Table S1 lists AmiC amino acids that are potentially involved in CNP binding, and the corresponding amino acids involved in the binding of hNPR-C to CNP as described by He *et al.* (33). Amino acids located within 4 Å of CNP in the binding sites of both hNPR-C and AmiC are shown schematically in the supplemental material (Fig. S1). A

total of 24 amino acids from AmiC and 21 residues from hNPR-C with equivalent physico-chemical properties are located in the same regions and may stabilize the binding of CNP to AmiC and NPR-C equivalently.

We also determined the virtual capacity of *P. aeruginosa* AmiC to bind natriuretic peptides (BNP and CNP) by molecular docking using AutoDock (34). Docking revealed that CNP can bind to AmiC at the dimer interface of the bacterial protein (See Fig. S2A, B in the supplemental material). The most relevant calculated binding site of CNP on AmiC requires 13 amino-acids, Arg64, Glu68, Ala90, Met92, Pro93, Glu96, Arg97, Asp99, Glu112, Tyr113, Pro115, Asn116 and Tyr366. Since these predictions were obtained by an *in silico* study, the involvement of each of these residues need to be validated by constructing and studying the 13 correspondent mutant proteins, which will be addressed in a future work. In contrast, we observed *in silico* that BNP has no affinity to the AmiC protein. The NPR-C antagonist isatin also appeared capable of binding to the AmiC dimer interface (Fig. S2C, D). In this case, the AmiC amino-acids involved in the recognition of isatin are predicted to be Ile71, Arg72, Val94 and Arg97. These amino acids are located in the same region involved as the putative CNP binding site, and one residue (Arg97) could play a key role since it is potentially interacting with both CNP and isatin.

Effect of CNP on the expression of the amidase operon in *P. aeruginosa.*

In *P. aeruginosa,* AmiC is considered as a sensor protein. In the absence of stimulation (basal condition), AmiC binds to the AmiR protein, an antitermination factor, which down-regulates the transcription of the *amiEBCRS* operon (35). Upon binding of acetamide AmiC releases AmiR, triggering the transcription of the whole *ami* operon (36). In order to verify that CNP could act in the same manner as acetamide on AmiC, we measured by qRT-PCR *amiB*, *amiC*, *amiE* and *amiR* mRNA levels 1 hour after exposure of the bacterium to CNP. The *amiC*,

226 *amiE*, *amiR* mRNA levels were significantly increased (2.97 ± 0.2, 3.66 ± 0.39, and 2.73 ±
227 0.67 fold, $p < 0.001$, respectively) after 1 hour of exposure to CNP (10^{-6} M) (Fig. 4), whereas
228 the amount of *lecB* mRNA, encoded by a gene adjacent to the *ami* operon, was not modified.
229 In contrast, BNP (10^{-6} M) has no significant effect on the whole *ami* operon transcriptional
230 activity (data not shown).
231
232 **AmiC binding with natriuretic peptide receptor agonists.**
233 In order to confirm that the action of CNP and isatin on *P. aeruginosa* is mediated directly
234 through AmiC, and is not an indirect effect, we investigated their binding to AmiC *in vitro*.
235 Recombinant AmiC was expressed in *E. coli*. We first confirmed the oligomeric state of
236 AmiC using native gel electrophoresis and analytical gel filtration (See Fig. S3 in the
237 supplemental material). These methods showed an apparent molecular weight of 120 ± 30
238 kDa and 136 ± 3 kDa, respectively. These results are most consistent with AmiC (protomer
239 MW: 45.5 kDa) forming a dimer with an irregular shape, as predicted by the model (Fig. S3).
240 We then tested the interaction of AmiC with natriuretic peptide receptor agonists and isatin
241 using microscale thermophoresis (Fig. 5A). AmiC bound to CNP tightly, showing a
242 dissociation constant (K_D) of 2.0 ± 0.3 μM (Fig. 5). In contrast, we observed that BNP
243 possessed no affinity for AmiC (Fig. 5A). Isatin could also bind to AmiC, although in this
244 case the interaction was not so strong, showing a K_D of 600 ± 200 μM (Fig. 5A and 5B).
245 Additionally, we measured the interactions of other natriuretic peptide receptor agonists.
246 sANP, a specific NPR-A agonist, showed a weak interaction with AmiC, which had clearly
247 not proceeded to completion at 900 μM (Fig. 5B), the highest concentration point that we
248 were able to assess. These data clearly predict that the K_D is greater than 600 μM. Conversely,
249 our initial experiments on osteocrin (a specific NPR-C agonist) showed a very strong
250 interaction with AmiC, apparently tighter than we were able to determine using the available

instrument. This indicates a K_D value below 100 nM. In the same way, cANF$^{4-23}$, another NPR-C specific agonist presented a K_D value of 40 ± 10 µM (Fig. 5).

Involvement of AmiC in CNP-regulated *P. aeruginosa* biofilm formation

In dynamic conditions, the biofilm formed by the PA14 *amiC*- strain appeared reduced in comparison to wild-type strain PA14 WT (Fig. 6A). Conversely, the morphology of the biofilm formed by the PA14 AmiC+ strain (PA14 containing the wildtype *amiC* gene plus extra *amiC* plasmid-borne copies) or by the PA14 EV strain carrying the empty vector was similar to that of the wild-type (data not shown). Complementation of the *amiC*- strain with the *amiC* gene carried by a vector restored entirely the ability of the bacteria to form a biofilm (Fig. 6A and 6B). The measure of the biofilm biovolumes revealed 64.5 ± 12.5 % reduction for the PA14 *amiC*- strain in comparison to the PA14 wild-type ($p < 0.001$) whereas the biovolume of the biofilm generated by the complemented strain is similar to that of PA14 wild-type (+13.7 ± 14.6 %) (Fig. 6B). The biofilm formed by the strain PA14 AmiC+ was slightly, but non significantly, enhanced (Fig. 6B).

We observed that the ability of CNP to reduce biofilm formation is abolished in the *amiC*- strain (Fig. 6A and 6C), and is restored using the complemented strain (-71.9 ± 12.7 %; ($p < 0.01$) (Fig. 6C). In contrast, BNP, which strongly reduced biofilm formation as well (-75.1 ± 9.9 %; ($p < 0.001$) (Fig. 6C), continued to have the same impact on biofilm formation on *amiC*- mutant strain (-70.8 ± 12.1 %; ($p < 0.05$) (Fig. 6C).

In parallel, since it has been previously shown that CNP also modifies *P. aeruginosa* virulence, we tested the effect of AmiC on cytotoxicity towards lung cells. We observed that whereas the PA14 wild-type strain showed an increase in cytotoxic activity after CNP exposure (+76.6 ± 17 %; $p < 0.001$), the *amiC*- strain did not significantly modify its cytotoxicity in the presence of CNP when compared with controls (*amiC*- strain without CNP

276 exposure) (+14.7 ± 6.0 %) (Fig. S4C). In accordance with these data, we observed that the
277 increased production of HCN triggered by CNP on PA14 wild-type strain disappeared in the
278 *amiC*- mutant strain (Figure S4D). It is interesting to note that the strain over-expressing
279 AmiC (AmiC+) strongly lost its ability to kill lung cells (Figure S4A), confirming a role for
280 AmiC in the regulation of *P. aeruginosa* virulence.
281

DISCUSSION

We have shown that *P. aeruginosa* is sensitive to micromolar concentrations of natriuretic peptides (i.e. BNP and CNP) and responds to these eukaryotic factors by a major increase in virulence (16, 17). Previously, the intra-bacterial cascade involving Vfr, PtxR, RhlR and LasR proteins, leading to a remodeling of the lipopolysaccharide (LPS) structure and an increase of HCN and exotoxin A production, was identified (16), but the nature of the *P. aeruginosa* natriuretic peptide sensors remained a central question.

P. aeruginosa is an opportunistic pathogen and in cystic fibrosis patients it is known to form biofilms in lung alveoli (2). As an exchange surface between air and blood, the alveolar epithelium formed by pneumocytes is particularly thin (0.2 µm). If bacteria are developing on this epithelium, they are certainly exposed to diffusible blood containing endocrine factors such as natriuretic peptides. These are also produced locally by endothelial cells (22), by lung airway epithelium cells and by nonciliated Clara cells (19). The growth of bacteria in biofilms is generally associated with a decrease of diffusible virulence factor synthesis (37). This assists in establishing a chronic infectious status, which progressively weakens the host leading to a potential lethal outcome (3). Conversely, an anticipated release of bacterial virulence factors, particularly when the bacterium is not protected by the biofilm, should trigger the host defence responses and the clearance of the pathogen and increase antibiotic sensitivity. Due to the effect on biofilm formation in *P. aeruginosa*, CNP and related molecules could potentially be interesting for therapy. CNP strongly decreased the biofilm formation activity of both *P. aeruginosa* PAO1 and PA14 strains confirming the hypothesis that virulence factor production and biofilm formation are inversely related. This is consistent with our previous results showing that CNP enhances cAMP production in *P. aeruginosa* (17). Indeed, cAMP and c-di-GMP synthesis appear to be antagonistically regulated in

bacteria. Whilst c-di-GMP promotes the growth of biofilms (23), cAMP prevents *P. aeruginosa* biofilm formation (38). The present results are also in agreement with the observation that CNP induces a rearrangement of the *Pseudomonas* LPS structure (17) and enhances *algC* mRNA synthesis (16), since LPS contributes to the bacterial surface properties and AlgC is involved in the synthesis of the LPS core (39).

In order to identify the potential natriuretic peptide sensor in *P. aeruginosa*, we started from the hypothesis that this protein should show structural homology with the binding domain of eukaryotic natriuretic peptide receptors. Van den Akker *et al.* (28) have shown that the binding domain of the eukaryotic natriuretic peptide receptor subtype A (NPR-A), a receptor which binds ANP and BNP, exhibits a type-I periplasmic binding protein fold and that the closest structural neighbour of this ANP binding domain is the AmiC protein from *P. aeruginosa*. Analysis of the crystal structure of the dimerized hormone binding domain of NPR-A and of the structure of the AmiC-AmiR complex showed that in NPR-A and AmiC, the same residues in helixes α3 and α7 interact respectively with ANP and AmiR. Furthermore, the pocket forming the ANP binding site on NPR-A overlaps with the recognition site of AmiR on AmiC (27, 28). In eukaryotes, NPR-A is known as a receptor-enzyme coupled to cGMP synthesis. However, CNP does not lead to an increase of cGMP in *P. aeruginosa* whereas it stimulates cAMP synthesis (17). Then, we looked for possible similarities between AmiC and human NPR-C (hNPR-C), the sole ANP and CNP eukaryotic receptor coupled to an adenylate cyclase activity (40). We observed *in silico* that hNPR-C and *P. aeruginosa* AmiC proteins present 19% identity and 26% similarity, confirming the structural homology of eukaryotic natriuretic peptides receptors and AmiC (27). The AmiC binding domain helix α3 is delineated by amino-acids 85 to 99 (41). In the present study, we noted that the binding of CNP to AmiC would occur in the same region; 6 of the 13 CNP binding amino acids (Ala90, Met92, Pro93, Glu96, Arg97 and Asp99) are in helix α3,

suggesting that CNP could enter into competition with AmiR for binding on AmiC. We compared all the amino acids putatively involved in the AmiC-CNP interaction to those observed in the interaction of CNP with NPR-C in eukaryotes (33). The physico-chemical properties of amino-acids involved in these two interactions (*i.e.* CNP/AmiC in bacteria and CNP/NPR-C in eukaryotes) showed a remarkably high level of conservation (this study). We determined that AmiC (like NPR-C) (40) is functionally expressed as a dimer reinforcing the hypothesis that AmiC could have a CNP binding activity.

In *P. aeruginosa*, the *amiC* gene appears highly conserved (99.57% sequence homology and total preservation of the amino acid sequence between PAO1 and PA14 strains) suggesting that a crucial role is played by this protein in this species. The *amiC* gene is encoded in an operon including the *amiL*, *amiE*, *amiB*, *amiC*, *amiR* and *amiS* genes (36) [www.pseudomonas.com]. AmiC activation by acetamide, its classical ligand in bacteria, is known to provoke the release of AmiR leading to the transcriptional activation of the whole *ami* operon (35, 41). We therefore hypothesized that, if CNP acts on AmiC in a similar fashion to acetamide, it should also induce the *ami* operon expression. This was confirmed by our observations. CNP actually induced *amiERC* transcription, and the specificity of this action was reinforced by the lack of effect of BNP on the *ami* operon transcription (data not shown). As mentioned elsewhere, *P. aeruginosa* AmiC appears functionally related to hNPR-C and it is interesting to note that, in eukaryotic cells, NPR-C preferentially binds to CNP with a higher affinity than to BNP (33). Such highly conserved specific recognition modes between eukaryotic and bacterial sensors have been previously observed in *Helicobacter pylori* for the human hormone somatostatin whose bacterial sensor can only recognize one agonist sub-type (42).

The issue of how CNP contacts AmiC in *P. aeruginosa* needs to be addressed, as AmiC is predicted to be located in the bacterial cytoplasm [www.pseudomonas.com]. This

means that CNP must enter into the bacterium before binding to AmiC. Such an assumption is conceivable since another eukaryotic peptide, dynorphin, was shown able to cross freely the membrane of *P. aeruginosa,* inducing an increased virulence (14). This behaviour was explained by the high percentage of basic and hydrophobic amino acid residues present in dynorphin (76%) (43). Similarly, CNP contains 73% basic or hydrophobic amino acids. Moreover, natriuretic peptides have been shown to form pores in phospholipid bilayers (44) and could therefore manage their own entrance into the bacterium. However, we cannot exclude that AmiC protein could, in some conditions, reach the *P. aeruginosa* inner membrane. Indeed, AmiC belongs to the type I periplasmic binding fold protein family and the Uniprot data base claims that AmiC is located in the periplasmic space [www.uniprot.org; reference P27017]. One protein being located in multiple bacterial compartments to undertake unrelated functions is not unprecedented. Indeed, the EF-Tu protein, which acts in the bacterial cytoplasm as a ribosomal elongation factor, was shown to migrate upon stress to the plasma membrane and acquires new functions as a sensor molecule (45). In *P. aeruginosa,* EF-Tu, after migration into bacteria membrane also behaves as a plasminogen binding protein (46). To support this hypothesis, we observed, using AmiC antibodies, that whilst AmiC protein is mainly located into the bacterial cytosol, a proportion of AmiC is associated with the inner membrane compartment (See supplemental material Fig. S6). In this case, we assumed that CNP is delivered to AmiC proteins that have reached the inner membrane through protein transporters, for example. To reinforce this hypothesis we observed that a protein encoded by the gene PA14_64270 (ortholog of PA4858 in PAO1) possesses a high structural similarity with AmiC, could virtually bind CNP, and is necessary for the CNP effect on bacterial biofilm (See supplemental material Fig. S5).

Although a couple of bacterial sensors for eukaryotic messengers have been identified (6), to date none of the bacterial sensors structurally identified possess a similarity with the

382 eukaryotic counterpart receptor. For example, *E. coli* QseC, the sensor protein for
383 epinephrine, is an histidine sensor kinase that twice crosses the bacterial membrane, and
384 which appears structurally very different from the G-coupled protein receptor (9, 47). In the
385 same vein, interferon-γ, which binds the eight transmembrane *P. aeruginosa* OprF protein
386 (48), in mammals activates a single transmembrane receptor. Since our data suggest that
387 AmiC and hNPR-C possess a homologous 3D-structure, and that CNP acts as an agonist on *P.*
388 *aeruginosa*, we undertook to study the pharmacological profile of AmiC, as happens in
389 eukaryotic receptor studies.

390 Results from our pharmacological studies carried out using $cANF^{4-23}$, a NPR-C agonist, and
391 isatin, an NPR-A/NPR-C antagonist (49) also support the hypothesis that AmiC acts as an
392 ortholog of eukaryotic NPR-C. *In silico* molecular modeling revealed that isatin binding to
393 AmiC would require only 4 amino acids but, as expected for an antagonist, these amino acids
394 are located in the potential CNP binding pocket of AmiC. The antagonist effect of isatin was
395 confirmed experimentally. Isatin had no intrinsic activity on the biofilm formation activity of
396 *P. aeruginosa* but inhibited the effect of CNP. Conversely, the artificial peptide $cANF^{4-23}$, a
397 specific NPR-C agonist in eukaryotes, was able to reproduce the effects of CNP on *P.*
398 *aeruginosa* global virulence on lung cells, as observed by Blier *et al.* (16). These data
399 reinforced the hypothesis that AmiC acts as a sensor for natriuretic peptides, but do not
400 exclude the possibility that these peptides bind to another protein that in turn affects AmiC. In
401 order to validate our hypothesis, we purified *P. aeruginosa* AmiC recombinantly produced in
402 *E. coli* and checked the interactions of CNP, BNP, isatin, osteocrin (an NPR-C agonist) (50),
403 $cANF^{4-23}$ (an NPR-C agonist) and sANP (an NPR-A agonist) (51) with AmiC. As expected,
404 AmiC bound strongly to CNP, showing a K_D of 2.0 ± 0.3 μM, consistent with the effective
405 concentrations of CNP on *P. aeruginosa*. In contrast, BNP does not interact with AmiC
406 suggesting that BNP acts on *P. aeruginosa* through another bacterial target, a hypothesis

strongly reinforced by the fact that BNP retains an effect on biofilm formation in the *amiC*-mutant strain (this study). Isatin also showed a specific interaction, although at a significantly higher concentration (600 ± 200 µM). As normal blood isatin concentrations are usually of the order of 0.3-1.3 µM (52), this implies that *in vivo*, isatin is unlikely to be at a sufficiently high concentration to antagonise the effects of CNP on AmiC. Finally, we attempted to test specific agonists of NPR-A and NPR-C, to confirm that AmiC reflects NPR-C specificity. sANP showed some interaction with AmiC, but this interaction was weak, and indeed was not complete at the highest ligand concentration available, indicating a K_D (likely considerably) in excess of 600 µM, explaining probably the weak effect of this peptide on bacteria cytotoxicity (this study). In contrast, initial experiments on osteocrin showed that it bound sufficiently strongly that it was beyond the limit of detection of our experiment (100 nM), and $cANF^{4-23}$ possesses a K_D in the same range as CNP. These observations suggest that AmiC does indeed show the same specificity as NPR-C, and is selective against NPR-A agonists. Finally, using an *amiC* deficient mutant strain and its complemented derivative, we physiologically validated the crucial role of AmiC sensor in CNP effects on *P. aeruginosa* virulence expression and biofilm formation.

The last puzzling question is the reason why a bacterium such as *P. aeruginosa* should express a sensor system for peptides which are naturally labile molecules only present in the inner medium of vertebrates. The fact that the CNP sensor should also be a binding site for isatin provides some clues on a possible explanation. Isatin, or indole-2,3-dione, is an interspecies signal molecule produced in large amounts by bacteria such as *Escherichia coli* (53). Until now, Pseudomonads were not thought to synthesize isatin or isatin related compounds but as shown by Lee *et al.* (54) and in the present study, *P. aeruginosa* can detect this molecule. Isatin is also produced in large amounts by vegetals where it is a precursor in auxin biosynthesis (55) and by mammalian tissues including lungs (56, 57). Therefore, in the

host, *P. aeruginosa* is regularly exposed to significant amounts of isatin. As is the case for GABA (15), it will gain an advantage by adapting its behavior in response to the host physiology. Nevertheless, even if this explanation is correct, the fact that AmiC showed common properties with the eukaryotic NPR-C, including CNP recognition, remains to be explained.

In conclusion, the present work provides the first demonstration that bacteria are not only sensitive to eukaryotic messengers but could express eukaryotic receptor-like structures to detect human hormones. The AmiC sensor protein acts as an ortholog of the eukaryotic receptor NPR-C, acting as a CNP/Isatin sensor in *P. aeruginosa* that modulates bacterial biofilm formation. Since the CNP hormone is produced in the lung, the effects of CNP on the biofilm formation activity of *P. aeruginosa* could represent a natural defense mechanism against lung colonization. Furthermore, a natriuretic peptide receptor agonist has been used as bronchodilator drug (58). This could on the one hand pose a risk of enhancing *P. aeruginosa* virulence; and on the other it may prevent biofilm formation. This opens up the tantalising prospect that compounds in development for other indications could be re-targeted for use against biofilms.

MATERIALS AND METHODS

Reagents and test substances.

The CNP peptide was obtained from Polypeptide (Strasbourg, France). Isatin and hBNP were purchased from Sigma-Aldrich (St Quentin Fallavier, France). Osteocrin, sANP and $cANF^{4-23}$ were synthesized by Dr J. Leprince (PRIMACEN Platform, University of Rouen, France). DMSO was purchased from Acros Organics (Geel, Belgium).

Bacterial strains and bacterial cultures.

Pseudomonas aeruginosa PAO1 was obtained from an international collection (17). *P. aeruginosa* MPAO1 was originally from Iglewski lab. A transposon library was constructed from the MPAO1 strain at the University of Washington (59). The *P. aeruginosa* PA14 was from Harvard Medical School (Boston, MA) (60) and kindly provided by the Biomerit Research Center (Univ. Cork, Ireland). All strains used in this work are listed in Supplemental material Table S2. All strains were grown at 37°C in Luria Bertani medium (LB). For treatment with CNP, an overnight culture was diluted to OD_{600} = 0.08 using a ThermoSpectronics (Cambridge, UK) spectrophotometer. CNP was added two hours after the onset of the culture, a time corresponding to the middle of the exponential growth phase. For all studies performed using isatin, because of its hydrophobicity this molecule was initially dissolved in a solution of dimethyl sulfoxide (DMSO) in water (5/95). The final concentration of DMSO in bacterial culture medium was kept under 0.2%. In this case, control experiments were conducted in the presence of the same final concentration of DMSO. The final bacterial density and the absence of contamination were controlled by plating.

Biofilm formation in dynamic conditions.

After 3 h of pre-culture in LB at 37°C, *P. aeruginosa* PA14 was inoculated at OD_{600} = 0.08 in LB medium and sub-cultured for 2 h. CNP (1 µM final concentration) was added and bacteria were grown for additional 3 h. Bacteria were then washed and adjusted to OD_{600} = 0.1 in 0.9% NaCl supplemented with CNP (1 µM). The bacterial suspensions were then used to study biofilm formation under dynamic conditions at 37°C in a three-channel flow cell as described by Bazire *et al*. (61). Briefly, each bacterial suspension was injected into a flow cell channel and bacteria were allowed to attach onto the glass coverslip for 2 h. A flow (2.5 ml/h) of LB medium containing CNP (1 µM) was then applied for 24 h. At the end of the experiments, the biofilms were stained with 5 µM Syto 61 Red dye or 5 µM SytoX (Molecular probes). Observations were made using a confocal laser scanning microscope (LSM 710 confocal laser-sanning microscope, Zeiss). The biofilm thicknesses and corresponding biovolumes were estimated by measuring field samples from at least 3 independent experiments using the COMSTAT software (62).

Biofilm formation in static conditions.

The static bacterial biofilm formation activity was determined after 24 h of development. Pre-cultures of *P. aeruginosa,* containing the pSMC2.1 plasmid harbouring the GFP gene, were grown overnight at 37°C. An aliquot of pre-culture (100 µl) was then added to 5 ml of LB medium supplemented with 400 µg/mL kanamycin. Tested molecules or the corresponding excipient were added after 2 hours of sub-culture. Three hours later, bacteria were collected by centrifugation (7,000 x *g*, 10 min). The supernatant was then removed and the pellets were resuspended in 25 ml of physiological solution (0.9% NaCl) and adjusted to OD_{600}= 0.1. Sterile glass slides, previously cleaned with 4% TFD4 in water (Dutscher, Brumath, France), were layered in Petri dishes and covered by the bacterial suspension. The slides were then incubated for 2 h at 37°C in static condition. At the end of the attachment period the

physiological solution was replaced by LB medium and incubated for 24 h at 37°C in static condition. The slides were then rinsed twice in 25 ml sterile phosphate buffered saline (PBS 0.1 M, pH=7.4) and bacteria were heat fixed. Biofilms were observed using a confocal laser scanning microscope (LSM 710, Zeiss). Images were treated using a 3 median filter and segmented using Zen® 2009 software (Zeiss). The volumes and thicknesses of the biofilms were estimated as described elsewhere (62). All 2D images are representative from 15 observations.

***In silico* studies.**

The STAMP software (31) was used within VMD (63) on a single computer. The GASH Structural Superposition software (32) was used on the web server (http://sysimm.ifrec.osaka-u.ac.jp/gash/). Potential ligand/protein interactions were investigated *in silico* by the molecular docking technique using the amidase sensor protein of *P. aeruginosa* AmiC (Protein Data Bank 1QO0). Essential hydrogen atoms, Kollman united atom type charges and solvation parameters were added with the aid of AutoDock tools (34). Affinity (grid) maps of 20X20X20 Å grid points and 0.375 Å spacing were generated using the Autogrid program (34). AutoDock parameter set- and distance-dependent dielectric functions were used in the calculation of the van der Waals and electrostatic terms, respectively. Docking simulations were made using the Lamarckian genetic algorithm (LGA). Initial position, orientation and torsions of the ligand molecules were set randomly. Each docking experiment was derived from three different runs that were set to terminate after a maximum of 1,000,000 energy evaluations. The population size was set to 100.

Quantitative reverse transcription-PCR (qRT-PCR) mRNA assays.

RNA extraction and quantification were realized as previously described (61) using bacteria grown for 3 h in LB. The primers employed are presented in supplemental material Table S3. The transcription level of 16S rRNA was used as the endogenous control. PCR reactions were performed in triplicate and the standard deviations were lower than 0.15 CT. Relative quantification of mRNA was obtained according to Bazire *et al.* (64) using the comparative CT ($2^{-\Delta\Delta CT}$) method (65).

Lung epithelial cells cytotoxicity tests.

The human A549 lung epithelial cell type II line (ATCC-CCL185TM) (American Type Culture Collection, Manassas, VA) was grown at 37°C in 5% CO_2 atmosphere in Dulbecco's modified Eagle's medium (DMEM, Lonza) supplemented with 10% fetal calf serum (Lonza) and 1% of penicillin and streptomycin (Penistrep, Lonza). For cytotoxicity assays, cells were seeded in 24 well plates at a final density of $3x10^5$ cells per well, and grown for 48 h before use. A minimum of 24 h before infection assays, cells were deprived of antibiotics and fetal calf serum by addition of a fresh serum- and antibiotics-free medium. For the assays, A549 cells were incubated for 2 h with control or pre-treated *P. aeruginosa* PA14 at a multiplicity of infection of 10. Bacterial cytotoxicity was determined by measurement of lactate dehydrogenase (LDH) release. LDH is a stable cytosolic enzyme that diffuses into the culture medium upon cell lysis. This marker of cytotoxicity was assayed using the Cytotox 96 enzymatic assay (Promega, Charbonnières, France) as previously described (17).

***P. aeruginosa* AmiC purification.**

To express *P. aeruginosa* AmiC in *E. coli*, a synthetic codon optimized gene was prepared (MWG Operon) with a leader sequence of MHHHHHHSSGVDLGTENLYFQS to provide a cleavable 6*His tag. This was cloned into the *Nco*I and *Hind*III restriction sites of the pET-

548 Duet1 vector (Novagen). This construct was transformed into Rosetta2 (DE3) cells
549 (Novagen), and grown in 500 mL of ZYM-5052 media (66) at 37°C until mid-log phase, and
550 then at 20°C overnight. Cells were harvested by centrifugation at 4,750 ×g for 30 min, and
551 resuspended in 20 mM Tris-HCl, 0.5 M NaCl, 20 mM imidazole pH 8.0 (buffer A). Cells
552 were lysed using a sonicator, and clarified by centrifugation at 20,000 × g. The protein was
553 purified using a 1 mL HisTrap crude FF column and a Superdex 200 16/600 hr column (GE
554 Healthcare), using an ÄKTAxpress system (GE Healthcare) at 4°C. Lysate was loaded over
555 the IMAC column at 0.25 $ml.min^{-1}$, and washed with buffer A. AmiC was eluted in buffer A
556 supplemented with 250 mM imidazole pH 8.0 and loaded onto the gel filtration column. The
557 protein was then eluted isocratically in 10 mM Hepes-NaOH, 0.5 M NaCl pH 7.0. DMSO was
558 added to the purified protein to 1% (v/v), and the protein was concentrated using a Vivaspin
559 20 centrifugal concentrator (Sartorius; 10 kDa molecular weight cut-off) at 4°C.
560
561 **Microscale thermophoresis.**
562 AmiC was labeled using the RED-NHS Labeling kit (NanoTemper Technologies). The
563 labeling reaction was performed according to the manufacturer's instructions in the supplied
564 labeling buffer applying a concentration of 20 μM protein (molar dye:protein ratio ≈ 2:1) at
565 RT for 30 min. Unreacted dye was removed with the supplied dye removal columns
566 equilibrated with MST buffer (50 mM Tris-HCl pH 7.5, 150 mM NaCl, 10 mM $MgCl_2$). The
567 label:protein ratio was determined using photometry at 650 and 280 nm. Typically, a ratio of
568 0.8 was achieved.
569 AmiC, either labelled (CNP, isatin, BNP and $cANF^{4-23}$) or unlabeled (sANP, osteocrin), was
570 adjusted to 100 nM with MST buffer (50 mM Tris-HCl pH 7.5, 150 mM NaCl, 10 mM
571 $MgCl_2$) supplemented with 0.05 % Tween-20. CNP, isatin, sANP or osteocrin were dissolved
572 in MST buffer supplemented with 0.05 % Tween-20. A series of 1:1 dilutions were prepared

in the identical buffer, producing ligand concentrations ranging from 13 nM to 434 µM (CNP), 3.12 µM to 3 mM (isatin), 892 nM to 1.8 mM (sANP), 28 nM to 450 µM (BNP), 68 nM to 1.1 mM (cANF$^{4-23}$) and 120 pM to 4 µM (osteocrin). For thermophoresis, each ligand dilution was mixed with one volume of AmiC, which leads to a final concentration of AmiC of 50 nM and final ligand concentrations at half of the ranges above. After 5 min incubation, followed by centrifugation at 10,000 × *g* for 10 min, approximately 4 µL of each solution was filled into Monolith NT Standard Treated Capillaries (NanoTemper Technologies GmbH). Thermophoresis was measured using a Monolith NT.115 or Monolith NT.LabelFree instrument (NanoTemper Technologies GmbH) at an ambient temperature of 25°C with 5 s/30 s/5 s laser off/on/off times, respectively. Instrument parameters were adjusted with 50 % LED power and 20-40% MST power. Data of three independently pipetted measurements were analyzed (NT.Analysis software version 1.5.41, NanoTemper Technologies) using the signal from Thermophoresis + T-Jump. Following data analysis, the thermophoresis signals were fitted to formula for K_D from the law of mass action:

$$f(c) = unbound + \frac{(bound - unbound) \times \left([AmiC] + c + K_D - \sqrt{([AmiC] + c + K_D)^2 - (4 \times [AmiC] \times c)}\right)}{2 \times [AmiC]}$$

Where *f(c)* is the observed thermophoresis signal, *unbound* is the signal in the absence of ligand (normalized to 0), *bound* is the signal at infinite ligand concentration, *c* is the concentration of ligand in the same units as AmiC concentration, and K_D is the dissociation constant. The data were fitted using GraphPad Prism version 5, and figures for thermophoresis were generated using this software. For cANF$^{4-23}$, incubation with AmiC resulted in a dose-dependent increase in AmiC fluorescence, which confounds the MST signal. This increase was therefore measured using the MST device, and the data fitted to the above equation. To confirm that the fluorescence increase was related to binding, samples were heated to 95°C for 10 min with 2% (w/v) SDS and 20 mM DTT, and retested: addition of cANF$^{4-23}$ no longer increased fluorescence.

Statistical analysis.

The non parametric Mann-Whitney test was used to compare the means within the same set of experiments.

Supplemental material figures and tables

Supplemental Table S1. List of amino acids potentially involved in the binding of CNP to NPR-C and AmiC.

Supplemental Table S2. List of Strains and plasmids used in this study.

Supplemental Table S3. Primers used in this study.

Supplemental Figure S1. 2D ligand interaction diagrams. 2D representation of the CNP surrounded by amino acids of hNPR-C (a) and AmiC (b) located within 4 Å of the peptide.

Supplemental Figure S2. Modelisation of AmiC sensor and CNP or isatin interactions by molecular docking approach.

Supplemental Figure S3. Analytical native gel electrophoresis and size exclusion chromatography**.**

Supplemental Figure S4. Involvement of AmiC protein on PA14 cytotoxicity.

Supplemental Figure S5. Involvement of the transporter PA14_64270 (gene PA14_64270) orthologs of the protein PA4858 in PAO1, in the effect of CNP on both biofilm and virulence activity.

Supplemental Figure S6. AmiC location using Dot-Blot analysis.

ACKNOWLEDGEMENTS

We wish to thank Magalie Barreau and Olivier Maillot for technical assistance. We wish to thank Christine Farmer for linguistic insight for this manuscript. T. Rosay is a recipient of a doctoral fellowship from the French Ministry of Research (MRE). This work was supported by grants from the Communauté d'Agglomération d'Evreux, the Conseil Général de l'Eure, European Union (FEDER n°31970), the French Association “Vaincre la Mucoviscidose” and the InterReg IVA PeReNE project.

REFERENCES

1. **Costerton JW, Stewart PS, Greenberg EP.** 1999. Bacterial biofilms: a common cause of persistent infections. Science **284:**1318-1322.
2. **Bjarnsholt T, Jensen PO, Fiandaca MJ, Pedersen J, Hansen CR, Andersen CB, Pressler T, Givskov M, Hoiby N.** 2009. Pseudomonas aeruginosa biofilms in the respiratory tract of cystic fibrosis patients. Pediatric pulmonology **44:**547-558.
3. **Hoiby N, Bjarnsholt T, Givskov M, Molin S, Ciofu O.** 2010. Antibiotic resistance of bacterial biofilms. International journal of antimicrobial agents **35:**322-332.
4. **Ashish A, Shaw M, Winstanley C, Ledson MJ, Walshaw MJ.** 2012. Increasing resistance of the Liverpool Epidemic Strain (LES) of Pseudomonas aeruginosa (Psa) to antibiotics in cystic fibrosis (CF)--a cause for concern? Journal of cystic fibrosis : official journal of the European Cystic Fibrosis Society **11:**173-179.
5. **Camilli A, Bassler BL.** 2006. Bacterial small-molecule signaling pathways. Science **311:**1113-1116.
6. **Lesouhaitier O, Veron W, Chapalain A, Madi A, Blier AS, Dagorn A, Connil N, Chevalier S, Orange N, Feuilloley M.** 2009. Gram-negative bacterial sensors for eukaryotic signal molecules. Sensors (Basel) **9:**6967-6990.
7. **Sperandio V, Li CC, Kaper JB.** 2002. Quorum-sensing Escherichia coli regulator A: a regulator of the LysR family involved in the regulation of the locus of enterocyte effacement pathogenicity island in enterohemorrhagic E. coli. Infection and immunity **70:**3085-3093.
8. **Sperandio V, Torres AG, Kaper JB.** 2002. Quorum sensing Escherichia coli regulators B and C (QseBC): a novel two-component regulatory system involved in the regulation of flagella and motility by quorum sensing in E. coli. Molecular microbiology **43:**809-821.
9. **Hughes DT, Sperandio V.** 2008. Inter-kingdom signalling: communication between bacteria and their hosts. Nature reviews. Microbiology **6:**111-120.
10. **Sperandio V, Torres AG, Jarvis B, Nataro JP, Kaper JB.** 2003. Bacteria-host communication: the language of hormones. Proceedings of the National Academy of Sciences of the United States of America **100:**8951-8956.
11. **Rasko DA, Moreira CG, Li de R, Reading NC, Ritchie JM, Waldor MK, Williams N, Taussig R, Wei S, Roth M, Hughes DT, Huntley JF, Fina MW, Falck JR, Sperandio V.** 2008. Targeting QseC signaling and virulence for antibiotic development. Science **321:**1078-1080.
12. **Hegde M, Wood TK, Jayaraman A.** 2009. The neuroendocrine hormone norepinephrine increases Pseudomonas aeruginosa PA14 virulence through the las quorum-sensing pathway. Applied microbiology and biotechnology **84:**763-776.
13. **Wu L, Estrada O, Zaborina O, Bains M, Shen L, Kohler JE, Patel N, Musch MW, Chang EB, Fu YX, Jacobs MA, Nishimura MI, Hancock RE, Turner JR, Alverdy JC.** 2005. Recognition of host immune activation by Pseudomonas aeruginosa. Science **309:**774-777.
14. **Zaborina O, Lepine F, Xiao G, Valuckaite V, Chen Y, Li T, Ciancio M, Zaborin A, Petrof EO, Turner JR, Rahme LG, Chang E, Alverdy JC.** 2007. Dynorphin activates quorum sensing quinolone signaling in Pseudomonas aeruginosa. PLoS pathogens **3:**e35.
15. **Dagorn A, Chapalain A, Mijouin L, Hillion M, Duclairoir-Poc C, Chevalier S, Taupin L, Orange N, Feuilloley MG.** 2013. Effect of GABA, a Bacterial Metabolite,

on Pseudomonas fluorescens Surface Properties and Cytotoxicity. International journal of molecular sciences **14:**12186-12204.

16. **Blier AS, Veron W, Bazire A, Gerault E, Taupin L, Vieillard J, Rehel K, Dufour A, Le Derf F, Orange N, Hulen C, Feuilloley MG, Lesouhaitier O.** 2011. C-type natriuretic peptide modulates quorum sensing molecule and toxin production in Pseudomonas aeruginosa. Microbiology **157:**1929-1944.
17. **Veron W, Lesouhaitier O, Pennanec X, Rehel K, Leroux P, Orange N, Feuilloley MG.** 2007. Natriuretic peptides affect Pseudomonas aeruginosa and specifically modify lipopolysaccharide biosynthesis. The FEBS journal **274:**5852-5864.
18. **Drewett JG, Garbers DL.** 1994. The family of guanylyl cyclase receptors and their ligands. Endocrine reviews **15:**135-162.
19. **Nakanishi K, Tajima F, Itoh H, Nakata Y, Hama N, Nakagawa O, Nakao K, Kawai T, Torikata C, Suga T, Takishima K, Aurues T, Ikeda T.** 1999. Expression of C-type natriuretic peptide during development of rat lung. The American journal of physiology **277:**L996-L1002.
20. **Nowak A, Breidthardt T, Christ-Crain M, Bingisser R, Meune C, Tanglay Y, Heinisch C, Reiter M, Drexler B, Arenja N, Twerenbold R, Stolz D, Tamm M, Muller B, Muller C.** 2012. Direct comparison of three natriuretic peptides for prediction of short- and long-term mortality in patients with community-acquired pneumonia. Chest **141:**974-982.
21. **Vila G, Resl M, Stelzeneder D, Struck J, Maier C, Riedl M, Hulsmann M, Pacher R, Luger A, Clodi M.** 2008. Plasma NT-proBNP increases in response to LPS administration in healthy men. Journal of applied physiology **105:**1741-1745.
22. **Suga S, Itoh H, Komatsu Y, Ogawa Y, Hama N, Yoshimasa T, Nakao K.** 1993. Cytokine-induced C-type natriuretic peptide (CNP) secretion from vascular endothelial cells--evidence for CNP as a novel autocrine/paracrine regulator from endothelial cells. Endocrinology **133:**3038-3041.
23. **Coggan KA, Wolfgang MC.** 2012. Global regulatory pathways and cross-talk control pseudomonas aeruginosa environmental lifestyle and virulence phenotype. Current issues in molecular biology **14:**47-70.
24. **Klinger JR, Tsai SW, Green S, Grinnell KL, Machan JT, Harrington EO.** 2013. Atrial natriuretic peptide attenuates agonist-induced pulmonary edema in mice with targeted disruption of the gene for natriuretic peptide receptor-A. Journal of applied physiology **114:**307-315.
25. **Potter LR, Abbey-Hosch S, Dickey DM.** 2006. Natriuretic peptides, their receptors, and cyclic guanosine monophosphate-dependent signaling functions. Endocrine reviews **27:**47-72.
26. **Holm L, Sander C.** 1995. Dali: a network tool for protein structure comparison. Trends in biochemical sciences **20:**478-480.
27. **van den Akker F.** 2001. Structural insights into the ligand binding domains of membrane bound guanylyl cyclases and natriuretic peptide receptors. Journal of molecular biology **311:**923-937.
28. **van den Akker F, Zhang X, Miyagi M, Huo X, Misono KS, Yee VC.** 2000. Structure of the dimerized hormone-binding domain of a guanylyl-cyclase-coupled receptor. Nature **406:**101-104.
29. **Pearl L, O'Hara B, Drew R, Wilson S.** 1994. Crystal structure of AmiC: the controller of transcription antitermination in the amidase operon of Pseudomonas aeruginosa. The EMBO journal **13:**5810-5817.
30. **He X, Chow D, Martick MM, Garcia KC.** 2001. Allosteric activation of a spring-loaded natriuretic peptide receptor dimer by hormone. Science **293:**1657-1662.

31. **Russell RB, Barton GJ.** 1992. Multiple protein sequence alignment from tertiary structure comparison: assignment of global and residue confidence levels. Proteins **14:**309-323.
32. **Standley DM, Toh H, Nakamura H.** 2005. GASH: an improved algorithm for maximizing the number of equivalent residues between two protein structures. BMC bioinformatics **6:**221.
33. **He XL, Dukkipati A, Garcia KC.** 2006. Structural determinants of natriuretic peptide receptor specificity and degeneracy. Journal of molecular biology **361:**698-714.
34. **Morris GM, Goodsell DS, Halliday RS, Huey R, Hart WE, Belew RK, Olson AJ.** 1998. Automated docking using a Lamarckian genetic algorithm and an empirical binding free energy function. Journal of Computational Chemistry **19:**1639-1662.
35. **Wilson S, Drew R.** 1991. Cloning and DNA sequence of amiC, a new gene regulating expression of the Pseudomonas aeruginosa aliphatic amidase, and purification of the amiC product. Journal of bacteriology **173:**4914-4921.
36. **Wilson SA, Wachira SJ, Drew RE, Jones D, Pearl LH.** 1993. Antitermination of amidase expression in Pseudomonas aeruginosa is controlled by a novel cytoplasmic amide-binding protein. The EMBO journal **12:**3637-3642.
37. **Balasubramanian D, Schneper L, Kumari H, Mathee K.** 2013. A dynamic and intricate regulatory network determines Pseudomonas aeruginosa virulence. Nucleic acids research **41:**1-20.
38. **Ono K, Oka R, Toyofuku M, Sakaguchi A, Hamada M, Yoshida S, Nomura N.** 2014. cAMP signaling affects irreversible attachment during biofilm formation by Pseudomonas aeruginosa PAO1. Microbes and environments / JSME **29:**104-106.
39. **Goldberg JB, Coyne MJ, Jr., Neely AN, Holder IA.** 1995. Avirulence of a Pseudomonas aeruginosa algC mutant in a burned-mouse model of infection. Infection and immunity **63:**4166-4169.
40. **Anand-Srivastava MB, Sehl PD, Lowe DG.** 1996. Cytoplasmic domain of natriuretic peptide receptor-C inhibits adenylyl cyclase. Involvement of a pertussis toxin-sensitive G protein. The Journal of biological chemistry **271:**19324-19329.
41. **O'Hara BP, Norman RA, Wan PT, Roe SM, Barrett TE, Drew RE, Pearl LH.** 1999. Crystal structure and induction mechanism of AmiC-AmiR: a ligand-regulated transcription antitermination complex. The EMBO journal **18:**5175-5186.
42. **Yamashita K, Kaneko H, Yamamoto S, Konagaya T, Kusugami K, Mitsuma T.** 1998. Inhibitory effect of somatostatin on Helicobacter pylori proliferation in vitro. Gastroenterology **115:**1123-1130.
43. **Marinova Z, Vukojevic V, Surcheva S, Yakovleva T, Cebers G, Pasikova N, Usynin I, Hugonin L, Fang W, Hallberg M, Hirschberg D, Bergman T, Langel U, Hauser KF, Pramanik A, Aldrich JV, Graslund A, Terenius L, Bakalkin G.** 2005. Translocation of dynorphin neuropeptides across the plasma membrane. A putative mechanism of signal transmission. The Journal of biological chemistry **280:**26360-26370.
44. **Kourie JI.** 1999. Synthetic mammalian C-type natriuretic peptide forms large cation channels. FEBS letters **445:**57-62.
45. **Dallo SF, Kannan TR, Blaylock MW, Baseman JB.** 2002. Elongation factor Tu and E1 beta subunit of pyruvate dehydrogenase complex act as fibronectin binding proteins in Mycoplasma pneumoniae. Molecular microbiology **46:**1041-1051.
46. **Kunert A, Losse J, Gruszin C, Huhn M, Kaendler K, Mikkat S, Volke D, Hoffmann R, Jokiranta TS, Seeberger H, Moellmann U, Hellwage J, Zipfel PF.** 2007. Immune evasion of the human pathogen Pseudomonas aeruginosa: elongation

factor Tuf is a factor H and plasminogen binding protein. Journal of immunology **179:**2979-2988.

47. **Xie W, Dickson C, Kwiatkowski W, Choe S.** 2010. Structure of the cytoplasmic segment of histidine kinase receptor QseC, a key player in bacterial virulence. Protein and peptide letters **17:**1383-1391.

48. **Sugawara E, Nestorovich EM, Bezrukov SM, Nikaido H.** 2006. Pseudomonas aeruginosa porin OprF exists in two different conformations. The Journal of biological chemistry **281:**16220-16229.

49. **Medvedev A, Crumeyrolle-Arias M, Cardona A, Sandler M, Glover V.** 2005. Natriuretic peptide interaction with [3H]isatin binding sites in rat brain. Brain research **1042:**119-124.

50. **Moffatt P, Thomas G, Sellin K, Bessette MC, Lafreniere F, Akhouayri O, St-Arnaud R, Lanctot C.** 2007. Osteocrin is a specific ligand of the natriuretic Peptide clearance receptor that modulates bone growth. The Journal of biological chemistry **282:**36454-36462.

51. **Olson LJ, Lowe DG, Drewett JG.** 1996. Novel natriuretic peptide receptor/guanylyl cyclase A-selective agonist inhibits angiotensin II- and forskolin-evoked aldosterone synthesis in a human zona glomerulosa cell line. Molecular pharmacology **50:**430-435.

52. **Mawatari K, Segawa M, Masatsuka R, Hanawa Y, Iinuma F, Watanabe M.** 2001. Fluorimetric determination of isatin in human urine and serum by liquid chromatography postcolumn photoirradiation. The Analyst **126:**33-36.

53. **Lee J, Jayaraman A, Wood TK.** 2007. Indole is an inter-species biofilm signal mediated by SdiA. BMC microbiology **7:**42.

54. **Lee J, Bansal T, Jayaraman A, Bentley WE, Wood TK.** 2007. Enterohemorrhagic Escherichia coli biofilms are inhibited by 7-hydroxyindole and stimulated by isatin. Applied and environmental microbiology **73:**4100-4109.

55. **Zou P, Koh HL.** 2007. Determination of indican, isatin, indirubin and indigotin in Isatis indigotica by liquid chromatography/electrospray ionization tandem mass spectrometry. Rapid communications in mass spectrometry : RCM **21:**1239-1246.

56. **Watkins P, Clow A, Glover V, Halket J, Przyborowska A, Sandler M.** 1990. Isatin, regional distribution in rat brain and tissues. Neurochemistry international **17:**321-323.

57. **Medvedev A, Buneeva O, Glover V.** 2007. Biological targets for isatin and its analogues: Implications for therapy. Biologics : targets & therapy **1:**151-162.

58. **Edelson JD, Makhlina M, Silvester KR, Vengurlekar SS, Chen X, Zhang J, Koziol-White CJ, Cooper PR, Hallam TJ, Hay DW, Panettieri RA, Jr.** 2013. In vitro and in vivo pharmacological profile of PL-3994, a novel cyclic peptide (Hept-cyclo(Cys-His-Phe-d-Ala-Gly-Arg-d-Nle-Asp-Arg-Ile-Ser-Cys)-Tyr-[Arg mimetic]-NH(2)) natriuretic peptide receptor-A agonist that is resistant to neutral endopeptidase and acts as a bronchodilator. Pulmonary pharmacology & therapeutics **26:**229-238.

59. **Jacobs MA, Alwood A, Thaipisuttikul I, Spencer D, Haugen E, Ernst S, Will O, Kaul R, Raymond C, Levy R, Chun-Rong L, Guenthner D, Bovee D, Olson MV, Manoil C.** 2003. Comprehensive transposon mutant library of Pseudomonas aeruginosa. Proceedings of the National Academy of Sciences of the United States of America **100:**14339-14344.

60. **Liberati NT, Urbach JM, Miyata S, Lee DG, Drenkard E, Wu G, Villanueva J, Wei T, Ausubel FM.** 2006. An ordered, nonredundant library of Pseudomonas aeruginosa strain PA14 transposon insertion mutants. Proceedings of the National Academy of Sciences of the United States of America **103:**2833-2838.

61. **Bazire A, Shioya K, Soum-Soutera E, Bouffartigues E, Ryder C, Guentas-Dombrowsky L, Hemery G, Linossier I, Chevalier S, Wozniak DJ, Lesouhaitier O, Dufour A.** 2010. The sigma factor AlgU plays a key role in formation of robust biofilms by nonmucoid Pseudomonas aeruginosa. Journal of bacteriology **192:**3001-3010.
62. **Heydorn A, Nielsen AT, Hentzer M, Sternberg C, Givskov M, Ersboll BK, Molin S.** 2000. Quantification of biofilm structures by the novel computer program COMSTAT. Microbiology **146 (Pt 10):**2395-2407.
63. **Humphrey W, Dalke A, Schulten K.** 1996. VMD: visual molecular dynamics. Journal of molecular graphics **14:**33-38, 27-38.
64. **Bazire A, Diab F, Taupin L, Rodrigues S, Jebbar M, Dufour A.** 2009. Effects of osmotic stress on rhamnolipid synthesis and time-course production of cell-to-cell signal molecules by Pseudomonas aeruginosa. The open microbiology journal **3:**128-135.
65. **Livak KJ, Schmittgen TD.** 2001. Analysis of relative gene expression data using real-time quantitative PCR and the 2(-Delta Delta C(T)) Method. Methods **25:**402-408.
66. **Studier FW.** 2005. Protein production by auto-induction in high density shaking cultures. Protein expression and purification **41:**207-234.

Figure legends

Figure 1. Biofilm formation by *Pseudomonas aeruginosa* PA14 exposed to C-type Natriuretic Peptide (CNP) or Brain Natriuretic Peptide (BNP) in dynamic condition. (A) COMSTAT analyses of biofilms of *P. aeruginosa* PA14 control (PA14) or exposed to CNP (10^{-6} M) or BNP (10^{-6} M). (✶✶✶ = $p < 0.001$). Data are the means of twelve samples from six independent experiments for control bacteria, ten samples from six independent experiments for CNP-exposed bacteria and six samples from two independent experiments for BNP-exposed bacteria. (B) 3D-shadow representations of the biofilm structures developed under dynamic condition by *P. aeruginosa* PA14 control, exposed to CNP or exposed to BNP at 37 °C for 24 h in LB broth. Biofilms were stained with the Syto 61 Red dye or SytoX dye and observed by confocal laser scanning microscopy.

Figure 2. Effect of antagonists and agonists of natriuretic peptide receptors. (A) 2D black and white images resulting from CLSM observations of MPAO1 24-h biofilms obtained in static condition after growth in control condition, exposed to CNP (10^{-6} M), exposed to isatin (10^{-5} M) or exposed to both isatin and CNP. (B) COMSTAT analyses of biofilms of *P. aeruginosa* MPAO1 exposed to CNP (+ CNP), exposed to isatin (+ Isa) or exposed both to isatin and CNP (+Isa + CNP). Data are the mean of three independent experiments for CNP exposition, and two independent experiments for isatin and isatin + CNP exposition. (✶✶✶= $p < 0.001$; NS: Not significantly different). (C) Cytotoxic activity of PA14 alone (control), PA14 exposed to NPR-C agonist $cANF^{4-23}$ (10^{-6} M) or PA14 exposed to NPR-A agonist sANP (10^{-6} M). The cytotoxic effect of the bacterium was determined by measuring lactate dehydrogenase (LDH) accumulation in the medium. Data are the means of nine samples from three independent experiments for $cANF^{4-23}$ and six samples from two independent experiments for sANP. ✶✶✶: Significantly different ($p< 0.001$). ✶✶: Significantly different ($p< 0.01$). ✶: Significantly different ($p< 0.05$).

Figure 3. Cartoon representation of AmiC (pdb:1PEA), in red, and hNPR-C (pdb:1JDP), in blue, superimposed using STAMP algorithm. (A) Overall superimposition of AmiC and NPR-C, shown in cartoon form. CNP peptide is colored green. (B) Superimposition by lobes of AmiC and hNPR-C. The lobe on the left corresponds to amino acids 8 to 123 and 261 to 338 of AmiC. The lobe on the right corresponds to amino acids 124

to 260 and 339 to 375 of AmiC. These images were made using VMD (Humphrey et al., 1996).

Figure 4. Effect of C-type Natriuretic Peptide (CNP) on expression level of genes from the *ami* operon. Expression levels of *ami* genes in PAO1-treated bacteria relative to those in PAO1 non-treated (control). RNAs were extracted 1 h after PAO1 exposure to physiologic solution (control) or CNP (10^{-6} M) and assayed by quantitative real-time reverse transcription-PCR (qRT-PCR). These data are the mean of two independent experiments. ✶✶✶ = $p <$ 0.001; NS: Not significantly different.

Figure 5. CNP, BNP , NPR agonists and isatin affinities for AmiC *in vitro*. Recombinant AmiC was fluorescently labeled and incubated with varying concentrations of natriuretic peptides receptor agonists and isatin(A). These mixtures were then analysed using by microscale thermophoresis. The results were normalized to a fitted zero for unbound AmiC, and the thermophoresis signal shown as parts per thousand. Addition of $cANF^{4-23}$ caused AmiC fluorescence to increase in a dose dependent fashion: this increase was used as the signal rather than thermophoresis, as the effect confounds the thermophoresis signal. The results were fit to the dissociation constant formula from the law of mass action. The fitted values for K_D are shown for isatin, BNP, sANP, $cANF^{4-23}$ and osteocrin (B). We showed that these compounds bound either too weakly (sANP), more tightly (osteocrin) or presented no interaction (BNP). For each compound tested, data are the mean of three independent experiments.

Figure 6. Involvement of AmiC protein on *P. aeruginosa* biofilm formation. (A) 3D-shadow representations of the biofilm structures developed by *P. aeruginosa* PA14 control (PA14), *amiC*- strain and *amiC*- complemented strain (*amiC*- Comp), not exposed to peptide or exposed to CNP (10^{-7} M) in dynamic condition, at 37 °C for 24 h in LB broth. Biofilms were stained with the SytoX and observed by confocal laser scanning microscopy. (B) COMSTAT analyses of biofilms of *P. aeruginosa* PA14 control, *amiC*-, *amiC*- complemented and AmiC+ strain. (C) COMSTAT analyses of biofilms of *P. aeruginosa* PA14 control, *amiC*- and *amiC*- complemented exposed to CNP (10^{-7} M) or to BNP (10^{-7} M) or neither of them. Data are the means of twenty-seven samples from eleven independent experiments for PA14 control, eleven samples from four independent experiments for PA14 exposed to CNP, nine samples from three independent experiments for PA14 exposed to BNP, nineteen

924 samples from seven independent experiments for *amiC*- control, twelve samples from four
925 independent experiments for *amiC*- exposed to CNP, eight samples from three independent
926 experiments for *amiC*- exposed to BNP, twenty four samples from six independent
927 experiments for *amiC*- Comp control and twelve samples from four independent experiments
928 for *amiC*- Comp exposed to CNP. Note that the wild-type (left), *amiC*$^-$ (middle) and *amiC*$^-$
929 Comp (right) strain values are set to 100% independently. ✶✶✶ = $p < 0.001$; ✶ = $p < 0.05$;
930 NS: Not significantly different.

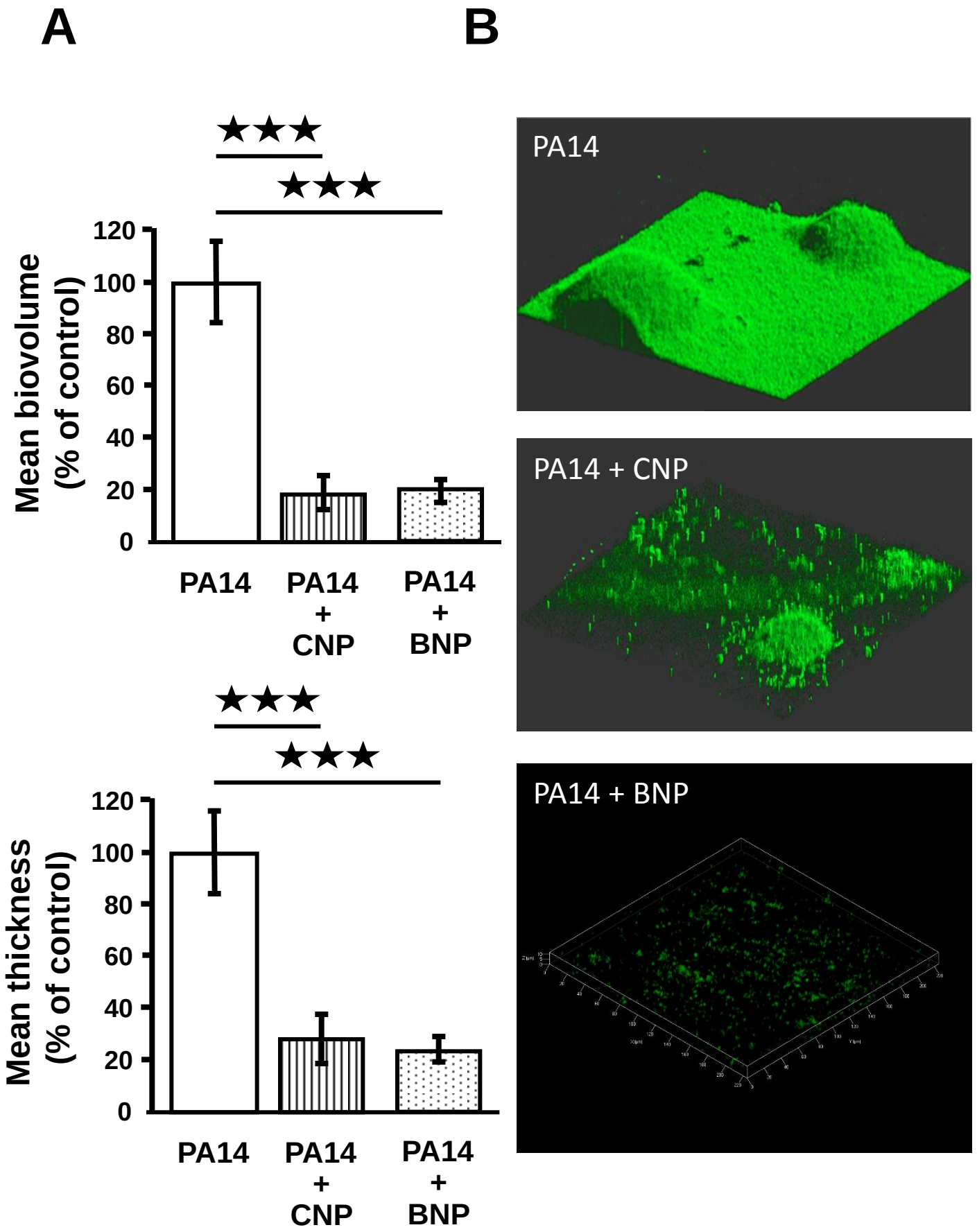
A
B
★★★
★★★
Mean biovolume (% of control)
120
100
80
60
40
20
0
PA14
PA14 + CNP
PA14 + BNP
★★★
★★★
Mean thickness (% of control)
120
100
80
60
40
20
0
PA14
PA14 + CNP
PA14 + BNP
PA14
PA14 + CNP
PA14 + BNP

Fig. 1

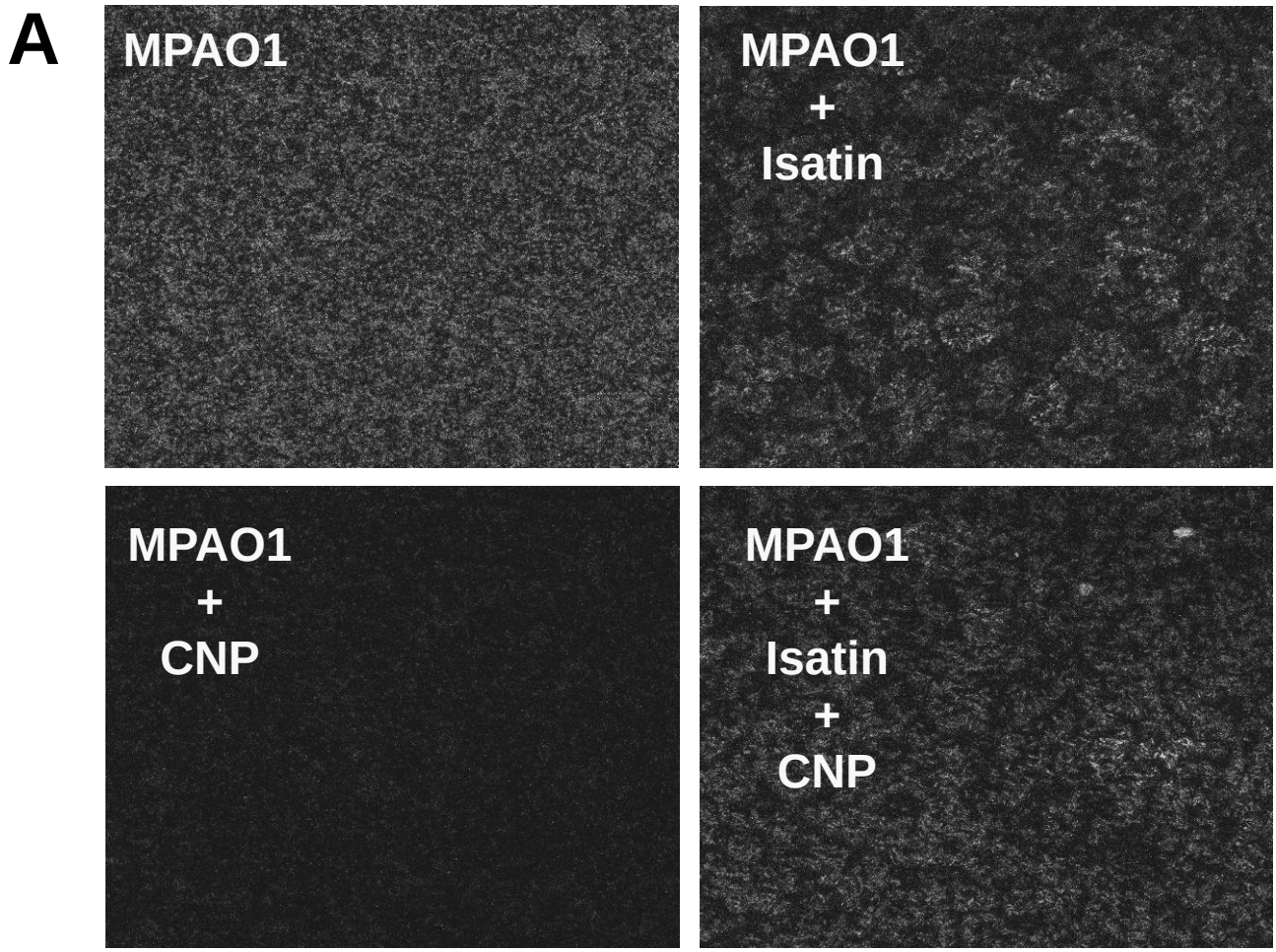
A
MPAO1
MPAO1
+
Isatin
MPAO1
+
CNP
MPAO1
+
Isatin
+
CNP
B
NS
NS
★★★
Mean biovolume (% of control)
140
120
100
80
60
40
20
0
MPAO1
+ CNP
+ Isa
+ Isa + CNP
NS
NS
★★★
Mean thickness (% of control)
140
120
100
80
60
40
20
0
MPAO1
+ CNP
+ Isa
+ Isa + CNP
C
★★★
★★
★
LDH (% of control)
200
150
100
50
0
PA14
+ sANP
+ cANF4-23

Fig. 2

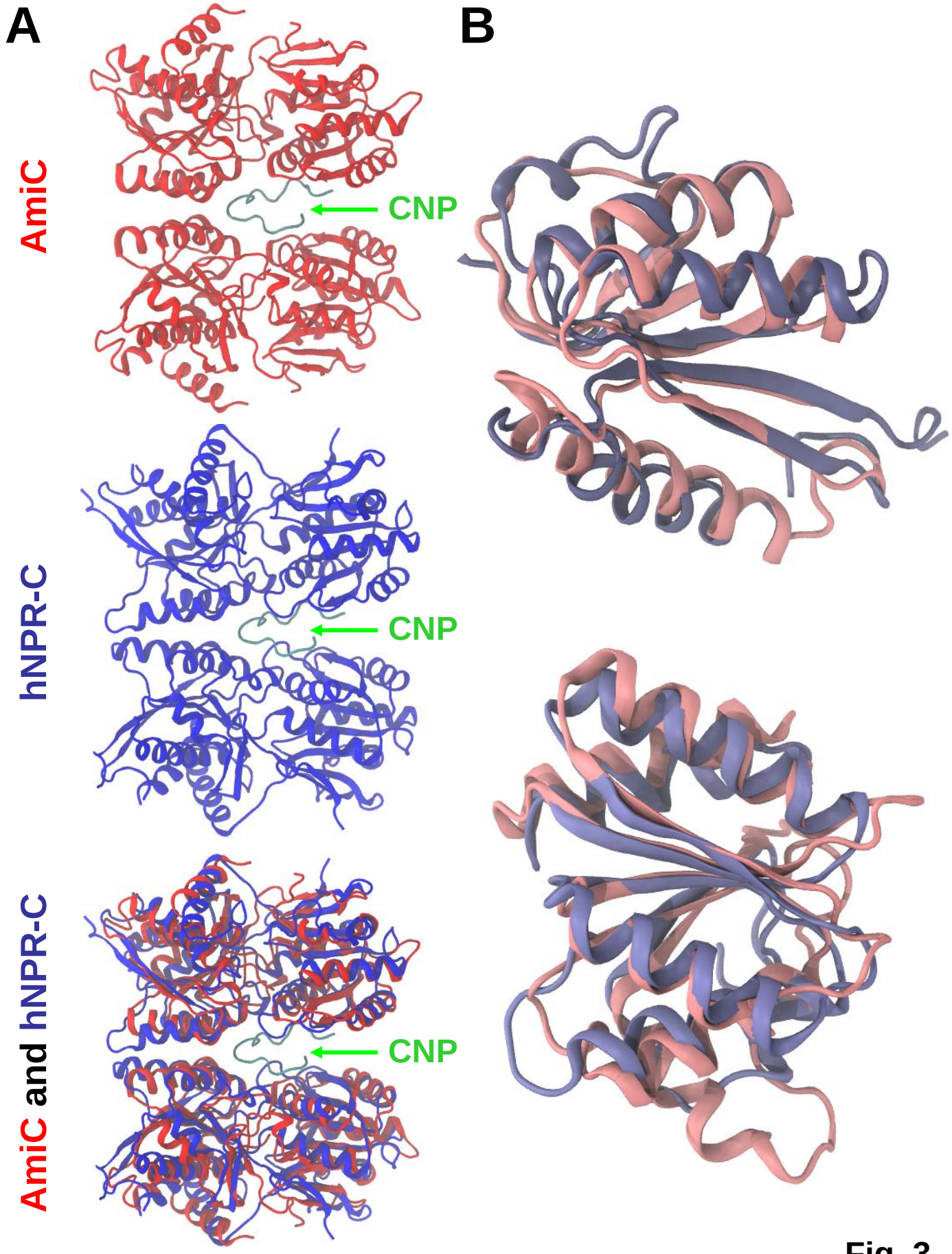

Fig. 3

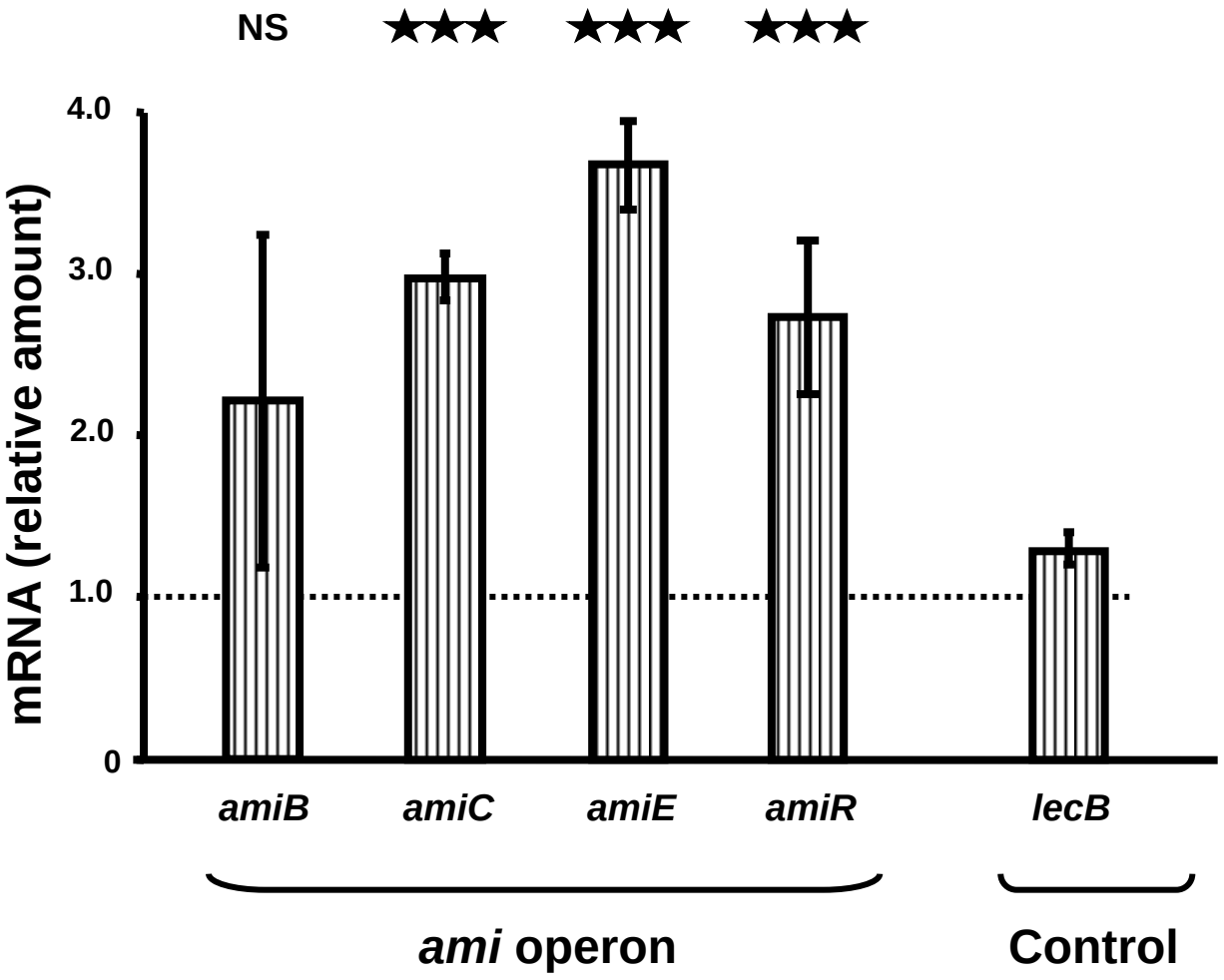
NS
★★★
★★★
★★★
4.0
3.0
2.0
1.0
0
mRNA (relative amount)
amiB
amiC
amiE
amiR
lecB
ami operon
Control

Fig. 4

A

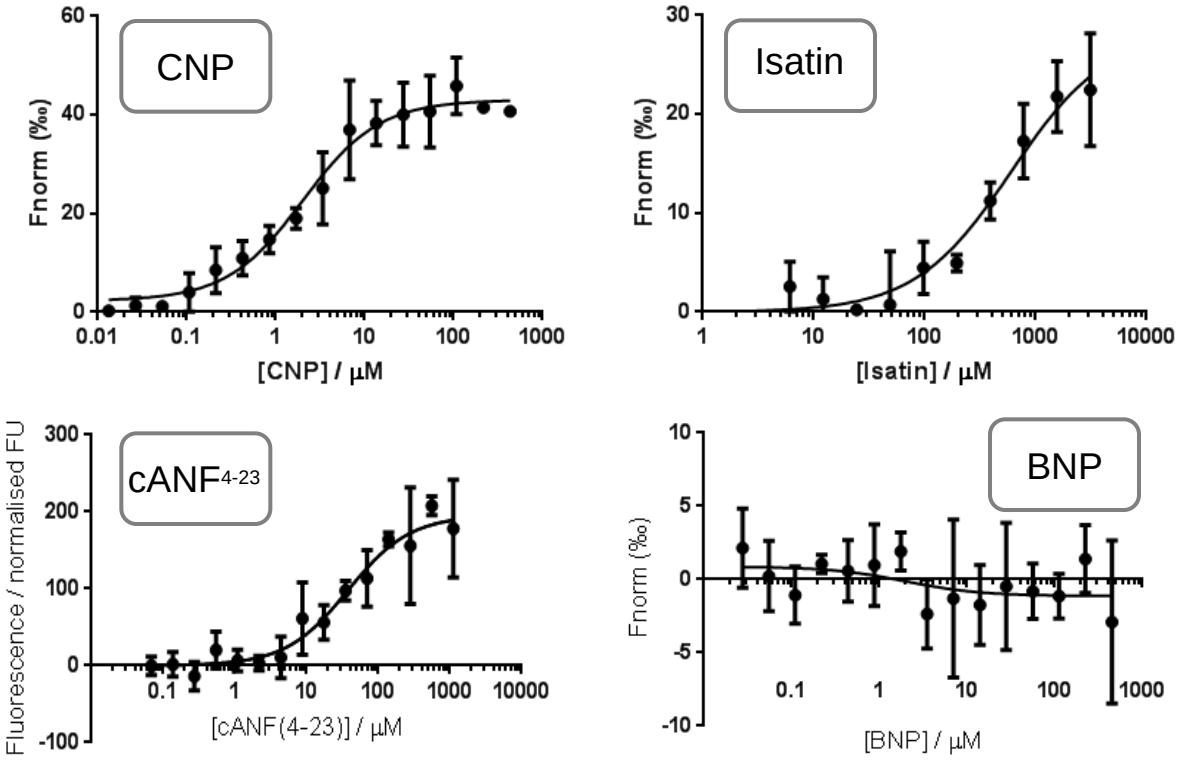

B

Ligands	Kd
CNP	2.0 ± 0.3 µM
BNP	No interaction
sANP (NPR-A agonist)	> 600 µM
Osteocrin (NPR-C agonist)	< 100 nM
cANF$^{4-23}$ (NPR-C agonist)	40 ± 10 µM
Isatin (NPR-A-NPR-C antagonist)	600 ± 200 µM

Fig. 5

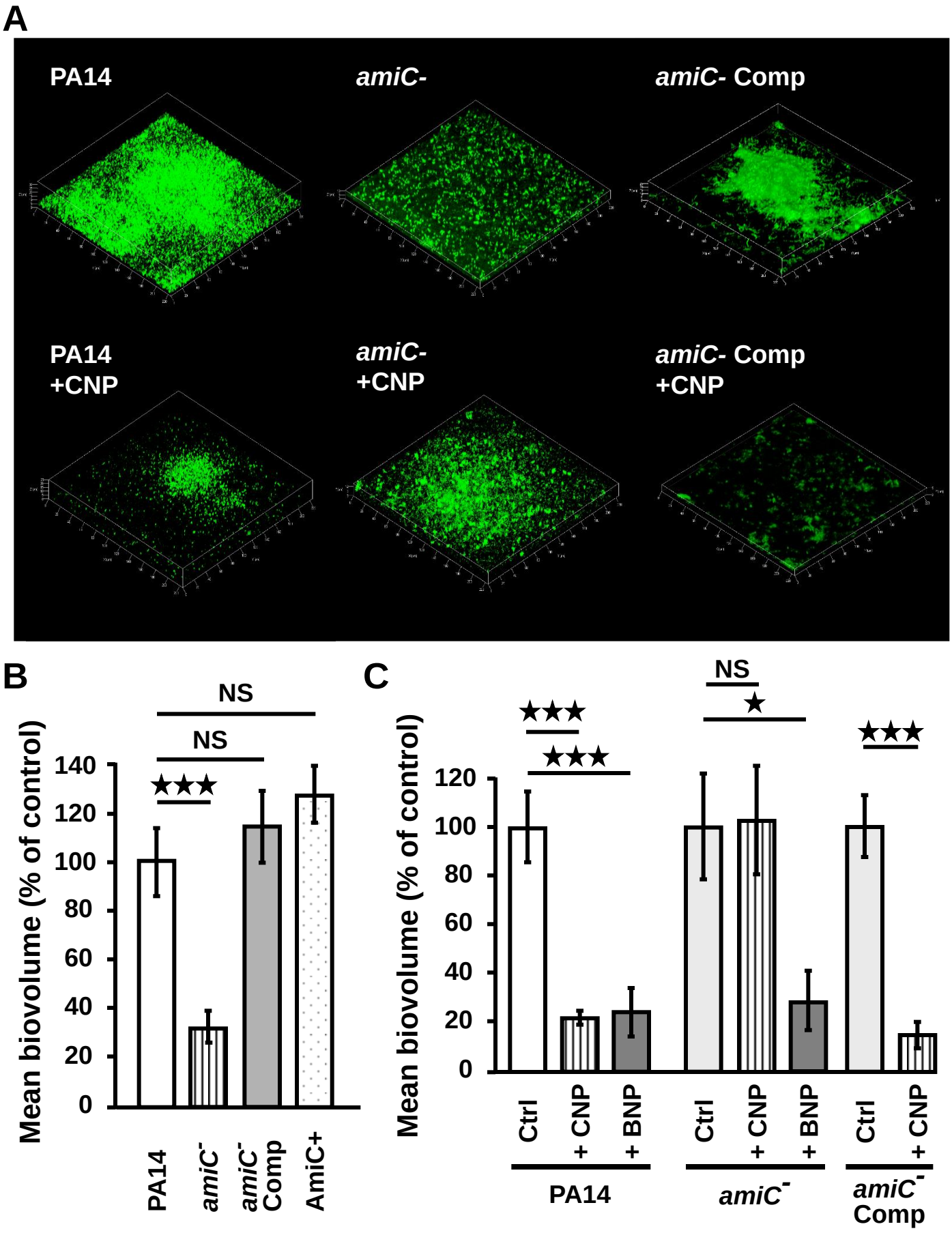
A
PA14
amiC-
amiC- Comp
PA14 +CNP
amiC- +CNP
amiC- Comp +CNP
B
NS
NS
★★★
Mean biovolume (% of control)
140
120
100
80
60
40
20
0
PA14
amiC-
amiC- Comp
AmiC+
C
NS
★
★★★
★★★
★★★
Mean biovolume (% of control)
120
100
80
60
40
20
0
Ctrl
+ CNP
+ BNP
Ctrl
+ CNP
+ BNP
Ctrl
+ CNP
PA14
amiC-
amiC- Comp

Fig. 6